Journal of Low Temperature Physics (2024) 216:165–174
https://doi.org/10.1007/s10909-024-03120-2

Tuneable Spectrometer for Submillimeter Astronomy Based on Silicon Fabry–Perot, Preliminary Results

T. Tollet[1] · L. Rodriguez[1] · V. Revéret[1] · A. Poglitsch[2] · L. Dussopt[3] · A. Aliane[3] · C. Delisle[1] · V. Goudon[3] · G. Lasfargues[3]

Received: 3 November 2023 / Accepted: 6 April 2024 / Published online: 12 May 2024

Abstract

We are studying and developing high-performance spectroscopy solutions in silicon technology in the framework of instrumental developments around the B-BOP bolometer arrays and in the continuation of the former developments of the Herschel space telescope instruments and in particular its photodetector array camera and spectrometer. The integration of multiwavelength spectroscopic capabilities close to the array of a cooled bolometer would make it possible to detect the interstellar medium continuum by scanning and to trace its evolution, particularly by the detection of characteristic lines such as the cooling line [CII] at 158 μm. In this paper, we present the first concept under development and the preliminary results obtained from our cryogenic optical test bench. This solution is a tunable Fabry–Perot cavity with silicon mirrors driven by a cryogenic piezoelectric mechanism with a nanometric step. Each mirror is a dielectric Bragg structure, a stack of quarter-wave layers of silicon and air providing high reflectivity without metal loss. This solution allows extremely accurate scanning around a targeted wavelength. The first prototype cannot be integrated on a focal plane as it stands, and future optimizations integrating miniaturized scanning systems will make the system much more compact.

Keywords Fabry–Perot · Tuneable spectrometer · Submm astronomy · Thin-film filters · Bragg stack

✉ T. Tollet
timothee.tollet@cea.fr

[1] CEA, CNRS, AIM, Université Paris Cité, Université Paris-Saclay, 91191 Gif-sur-Yvette, France

[2] Max-Planck Institut für extraterrestrische Physik, Garching bei Munich, Germany

[3] CEA-LETI, Université Grenoble Alpes, Grenoble, France

1 Introduction

The work presented in this paper takes place in the context of the development of a detector and its integrated functions for the study of the interstellar medium (ISM). A number of phenomena that govern the evolution of the ISM and lead to star formation are still not fully understood because they are so difficult to observe, particularly in the submillimeter range. This is mainly due to the fact that the atmosphere absorbs a large proportion of the radiation in this band, forcing astronomers to send instruments into orbit to gain access to all the ISM's emissions. In addition, the light emitted by these areas of the galaxies is very weak, so the instruments have to be extremely sensitive in order to detect it. Furthermore, the interest in studying these zones in spectroscopy is great because a certain number of emission lines make it possible to trace the different physicochemical phenomena. This is the case for the [CII] cooling line at 158 µm, which is a good tracer of the evolution of several phases of the ISM [1]. The detector we are designing for this purpose is a continuation of the development of the PACS instrument of the Herschel Space Telescopes [2]. This technology, named B-BOP (magnetic field (B) explorer with BOlometric Polarimeter), is a cryogenic high-sensitivity bolometric detectors in the 100–400 µm range, integrating imaging and polarimetry [3], and the integration of the spectroscopic capability is being studied.

The work presented here focuses on the development of this new capability for B-BOP. We are aiming to develop a compact lossless medium resolution spectrometer whose geometry and electromagnetic properties are compatible with this type of detector. For this purpose, we have chosen to focus on technologies based on the Fabry–Perot interferometry. This kind of interferometer has no influence on the polarization of the light and retains the spatial information as long as the mirrors are flat and the beam remains collimated. A Fabry–Perot (FP) is composed of two parallel mirrors perpendicularly positioned to the propagation direction of the incident wave. The light travels back and forth in the cavity and interferes constructively in transmission at the output of the cavity for selected wavelengths. The response in transmission of an ideal FP interferometer depends on the mirror properties (their reflection and absorption coefficients), the optical size of the cavity L, the wavelength of the incidence light, and the angle of incidence.

An ideal FP therefore transmits a comb of wavenumber in which all orders n are directly dependent on the cavity size, and with the fundamental wavelength that is equal to twice the cavity size. The orders transmitted by a FP are the λ_n such that:

$$\lambda_n = \frac{2L}{n}$$

Here the full width at half-maximum (FWHM) depends only on the reflection coefficient of the mirrors. The Finesse F is an effective way of assessing the performance of a FP. It quantifies the average number of round trips a photon makes in the cavity before exiting [4]. In the ideal case, the finesse can be defined by the reflection finesse $F_{\mathrm{R}} = \frac{\Delta\lambda}{\delta\lambda}$ only, where $\Delta\lambda = \frac{\lambda}{n}$ is the free spectral range (FSR) and $\delta\lambda$ the FWHM.

In practice, the finesse is affected by the flatness and the parallelism defects, and the effective finesse F_E can approximated by:

$$\frac{1}{{F_E}^2} = \frac{1}{{F_R}^2} + \frac{1}{{F_D}^2}$$

where F_D is the defect finesse that takes under consideration all the defects and deformations that can occur on the mirror plates, such as roughness defects, parallelism errors or spherical deformations.

This means that any degradation of flatness, surface or parallelism between the two mirrors, degrades the resolution of the transmitted peaks. Our objective is to build a mid-resolution compact FP interferometer with the least possible absorption, that is capable of transmitting several wavelengths close to each other. To develop such a tunable FP, we choose to modify the cavity size by scanning one of the mirrors.

2 The Concept of Bragg-Mirror Fabry–Perot

2.1 Design of the Mirrors

From the 1960s onwards, the use of mesh filters was adapted to design interference filters and Fabry–Perot interferometers for the far infrared [5–7]. These spectrometers are relatively simple to set up and they reach very high resolving powers. In these FPs, each mirror is a mesh or a metal grid whose geometric parameters are chosen to adapt the impedance to obtain good reflective properties. To date, almost exclusively metal mesh FPs have been used on space observation missions in the field of far-infrared and submm, notably on the instruments of the infrared space observatory (ISO) [8] or on the SOFIA airborne telescope [9, 10]. However, the major weakness of these FPs is that their efficiency does not exceed 60%, due to metal losses in the mesh mirrors. In the visible and infrared ranges, multilayer interference filters made from dielectric materials are used for spatial spectroscopy applications [11]. However, deposition manufacturing techniques are no longer applicable to multilayer stacks designed for longer wavelengths. Fabry–Perot projects using silicon deposition and etching technologies combined with metal meshes have recently emerged, expecting high performance and much lower absorption in reflectors than common FP. This is the case, for example, with the cryogenic FPs developed for astrophysics applications by Cornell University (USA), in which a thick multilayer substrate is deposited and etched directly onto gold mesh layers [12].

As part of the S. Bounissou thesis work [13] and in collaboration with teams at CEA/Leti, we propose a Fabry–Perot whose mirrors are entirely dielectric, based on the model of multilayer filters. These mirrors, known as Bragg reflectors [14], are stacks of three dielectric layers: silicon-vacuum-silicon as shown in Fig. 1. The silicon layers used in this concept are made from high resistivity float zone (HRFZ) silicon wafers manufactured at CEA/Leti. This crystalline silicon is extremely pure,

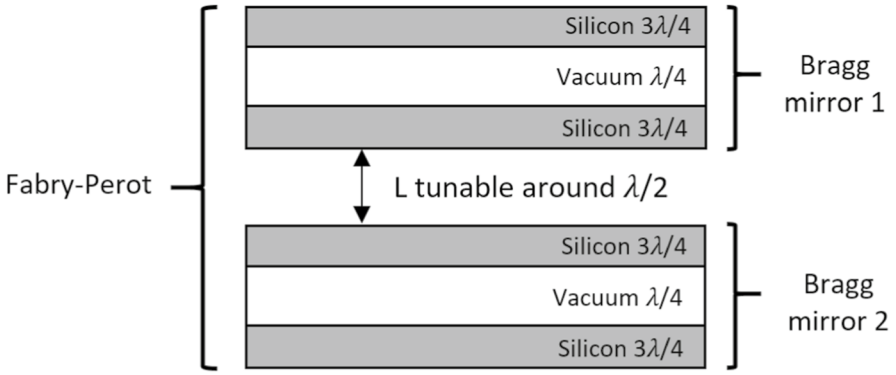

Fig. 1 Scheme of the scanning Bragg mirror Fabry–Perot concept

and thus highly resistive in our wavelength range. Moreover, owning to precise machining, we can achieve great precision in terms of thickness and flatness.

The principle of Bragg reflection is that the layers of the stack are quarter-wave thick and due to the alternation of high and low optical indices, constructive interference occurs in reflection. The combination of the lossless property of the crystalline silicon layers with the structuration in quarter-wave stack allows reaching very high reflectivity over a wide band of wavelengths.

For feasibility reasons, we are targeting transmitted wavelength around 320 µm. In fact, the layers composing our device are made of pure crystalline silicon and this is technically difficult to manufacture and handle thinned-layers with thicknesses less than 50 µm.

However, the principle we demonstrate in this paper for wavelengths around 320 µm remains identical to the one we would implement for a FP transmitting at 158 µm. The layers used here are 70.2 µm thick ($3\lambda/4$) for silicon and 80 µm thick ($\lambda/4$) for vacuum. The theoretical response was calculated on the model basis of the matrix theory of thin-films developed by Abelès [15], and is plotted below on Fig. 2. It shows that this mirror reflects more than 95% of the light on a range of almost 100 µm around 320 µm.

2.2 The Fabry–Perot Cavity

The Bragg mirrors allow us to have a high reflectivity in the targeted range but at a price. As shown in Fig. 2, there are many transmission zones, which has an impact on the response of the FP. In fact, we no longer expect a simple comb of wavelengths at the output of the FP, but rather a much more complex structure with Fabry–Perot peaks separated by fairly wide transmission zones. In addition, half of the orders (the even ones) are hidden in the reflective Bragg structures.

With this type of FP, the definitions of the FSR and thus the finesse mentioned above are no longer valid because the zones between the orders are no longer zones of pure reflection. However, we can consider that the FSR is reduced and therefore the finesse is poorer. But this is not of major importance because for an astrophysics

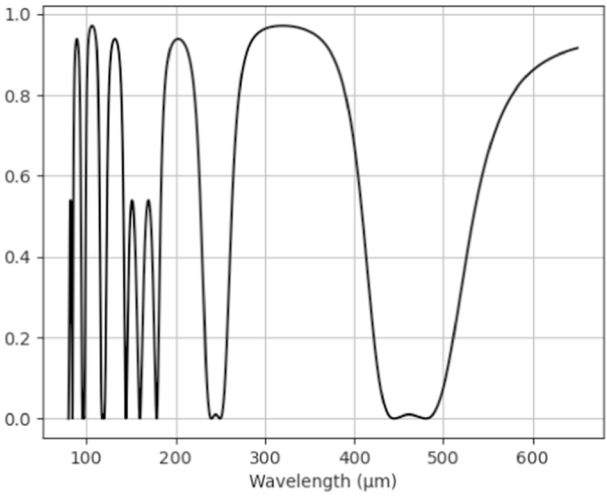

Fig. 2 Simulated reflectance of a three layer Bragg stack made of crystalline Si and vacuum

spectrometer, the spectrum is filtered relatively finely around the peak, generally using other interference filters with lower resolution. This is why, in what follows, we quantify the performance of our FP with a quantity that we call resolution $R = \frac{\lambda}{\delta\lambda}$, which depends exclusively on the wavelength of the peak and its FWHM. As previously mentioned, the value of the measured resolution is strongly correlated with the flatness of the assembled mirrors and of the roughness of the silicon sheets.

In 2019, the high performance of this concept was proven with a Bragg mirror FP with a fixed cavity of 160 μm. This first sample reached more than 98% efficiency for a resolution of more than 180. Our objective is now to be able to scan the cavity between the two mirrors to transmit several wavelengths close to each other with the same interferometer.

3 The Prototype of Scanning Bragg Fabry–Perot

The prototype we developed consists of a three piezoelectric actuators mechanism that adjusts the parallelism of the Fabry–Perot and scans the cavity. We designed this whole setup to operate under cryogenic vacuum conditions.

In Fig. 3 above, we fixed the mobile mirror on the blue part connected to the piezo mechanism and the other mirror on the bracket in front of the first one. The challenges of this experiment are first reaching a good parallelism of the mirrors before starting the vacuum and cold operations, and then finding back the initial parallelism and adjusting it by varying the tip and tilt of the mechanism under those harsh conditions. Many calibration and characterization operations, both optical and thermal, are thus necessary before performing spectral measurements of the tuneable FP.

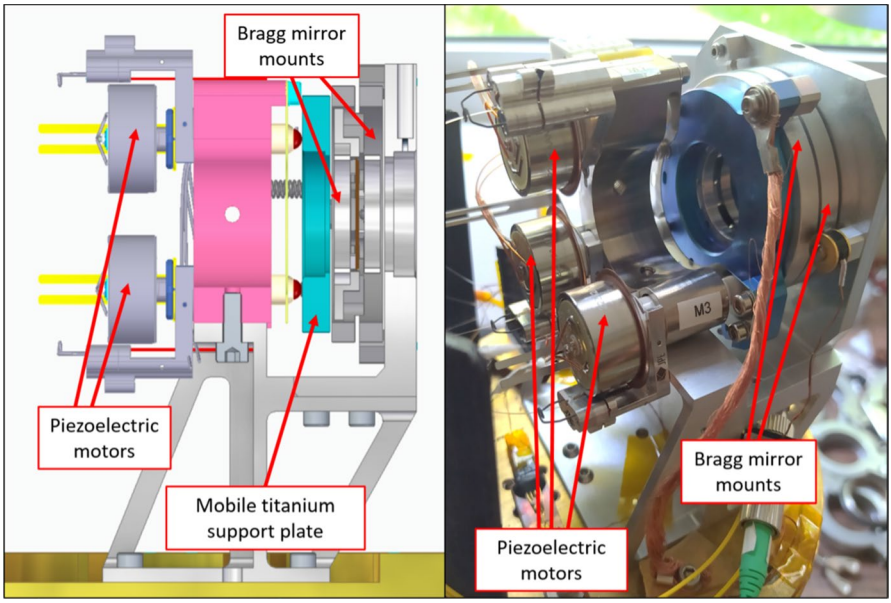

Fig. 3 3D cut of the assembly of the scanning Bragg mirror prototype (left) and picture of the full setup of scanning FP on the plate of the cryostat (right)

4 Results

The measurements were performed with a cryogenic Martin-Pupplet fourier transform spectrometer (FTS) with a 10 cm travel. The signal is acquired by a bolometer cooled down to 300 mK allowing us to get high resolution and low noise interferograms. Our optical samples are placed in the optical path between the FTS and the bolometer. For each spectrum shown below, many interferograms were acquired with the sample in the path and a second batch of measurements was made without the sample, for reference. Therefore, we can eliminate the spectral signature of the test bench environment and retrieve the absolute spectral efficiency of our sample.

Owning to a measurement of the single silicon sheet used for the Bragg mirrors, we have been able to determine its thickness precisely and thus feed the theoretical model with the spectral response of the two Bragg mirrors that we measured on the FTS at 77 K.

The measured spectra of those mirrors are similar to those of simulation (Fig. 4), they have high reflectivity (more than 95%) over a wide range of wavelengths. We then measured the response of the scanning FP with those two Bragg mirrors and saved the spectra for four different cavity sizes to get four different transmission peaks at 310 µm, 320 µm, 330 µm and 340 µm. To begin with, the first series of measurements was carried out with the sample kept at room temperature in order to simplify the mirror-paralleling operations. The rest of the optical bench was kept at cryogenic temperature. Figure 5 below shows the four

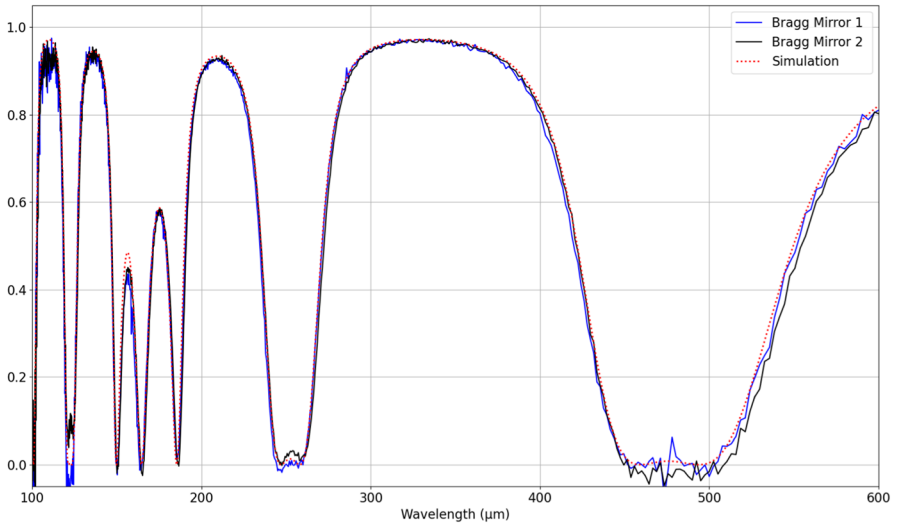

Fig. 4 Spectral reflection of the two Bragg mirrors used for the scanning FP measured in the FTS, in black and blue, compared to the theoretical response, in red (the same as plotted on Fig. 2) (Color figure online)

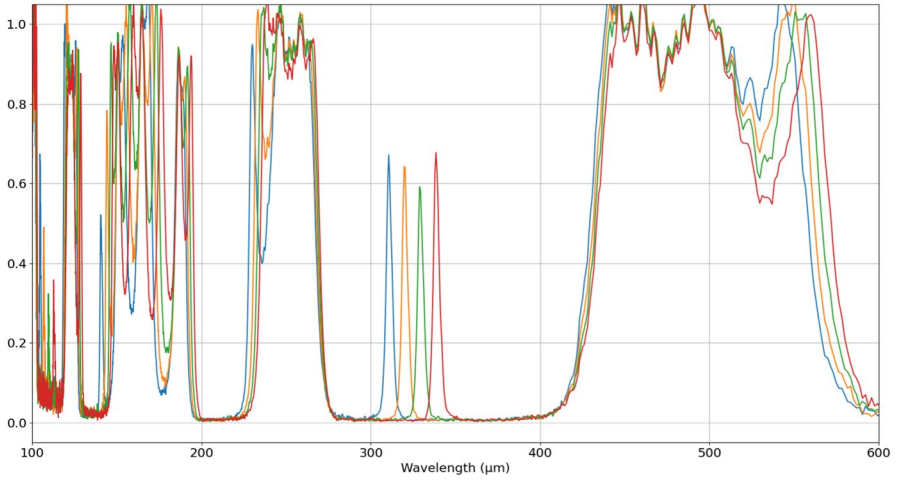

Fig. 5 Transmission spectra of the scanning FP for the four cavity sizes

spectra obtained with the scanning FP. By changing the cavity size by a known distance, we shift the position of the transmitted peak in accordance with the model.

With the same numerical model used for the Bragg mirrors, we can compare the performance of our interferometer with the theoretical simulation. Figure 6

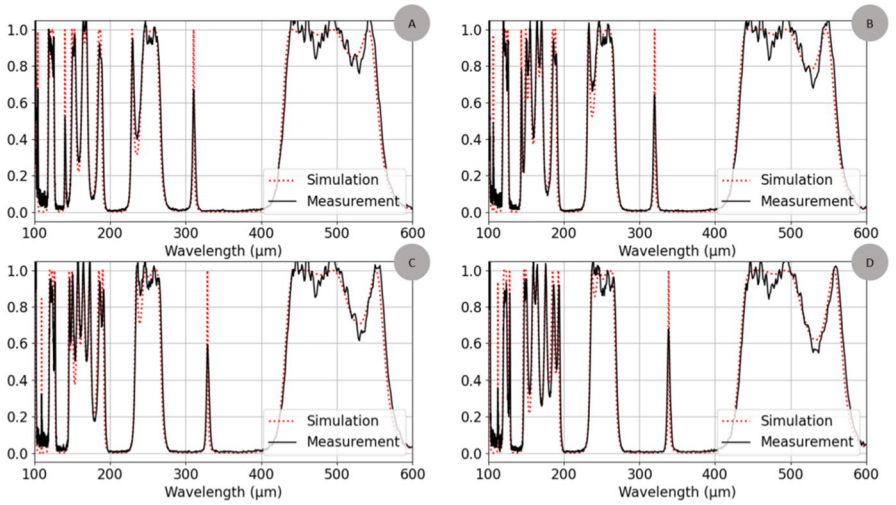

Fig. 6 Superposition of the measured spectra (black) with the simulation for the four spectra (red). **A**, **B**, **C** and **D** are the spectra for the FP at 310 μm; 320 μm, 330 μm and 340 μm respectively (Color figure online)

shows that the experimental measurements fit perfectly with the theory for the four positions. Nevertheless, the efficiencies of the transmitted wavelengths are lower than those of the simulated spectra. We summarize the efficiency and resolution of each peak of FP in the Table 1 below, and compare them with the expected performance.

As shown in the table above, the performances of the transmitted peaks are lower than expected. This can be explained by several factors. Most likely, in addition to the possible small parallelism defects, the Bragg stack are slightly deformed by the way they are assembled on their mounts (several microns of wedge). Even those small deformations have a big impact on the shape of the peak. This hypothesis has been confirmed by Fizeau interferometry measurements. We have seen large deformations, which, according to the work of S. Bounissou, must remain below 1 μm in amplitude to maintain maximum performance.

Table 1 Performance of the four transmitted peaks of FP. We calculated the expected resolutions from the theoretical model for a perfect Bragg mirror FP, plotted in red in Fig. 6

Wavelength μm	Measured resolution	Expected resolution	Efficiency %
310.8	79	180	68
320.1	84	210	66
329.3	80	216	60
338.7	86	211	69

5 Conclusion and Future Work

In conclusion, we succeeded in building a silicon Bragg mirror FP that scans a wide wavelength band in the submillimeter range with a high precision. We have demonstrated by measurement that Bragg mirrors perform very well both at room temperature and at 77 K and that their response is perfectly consistent with theory. Finally, we carried out measurements at room temperature of our FP at four different wavelengths, achieving resolutions greater than 80 and transmittances between 60 and 70%.

The next step is to optimize the assembly of the Bragg mirrors in order to reduce the deformations down to less than 1 μm of wedge. We have several ways to reduce the stress in the sheets. The first one is to avoid molecular adhesion between the sheets because it maintains and amplifies the stress and mechanical constraints in the stack. Another thing to do is to add a silicon spacer on the outer surface of each of the two silicon mirrors. These spacers will absorb the mechanical stress of the mechanical mount and transmit it in a much more spread-out manner to the silicon layer. Once these adjustments have been made, we will be able to repeat FP measurements at several wavelengths at room temperature, then at 77 K and 4 K to obtain performances close to the theoretical ones.

In the longer term, we plan to adapt this scanning Bragg mirror FP principle to much more compact scanning technologies such as MEMS, so that they can be more easily integrated into the focal plane of detectors.

Acknowledgements This work has been partially supported by the LabEx Focus ANR-11-LABX-0013.

Author Contributions T.T. wrote the main manuscript text. T.T. A.P. and L.R. performed the measurements presented in the paper. T.T. A.P. L.R. and V.R. processed and analyzed the data. C.D. designed and prepared the measurement setup. A.A. V.G. and G.L. manufactured the silicon technologies presented in the paper. T.T. L.R. V.R. L.D. and A.A. took part in the design and the development of the concept of spectrometer. L.R. V.R. and A.P. reviewed the manuscript.

Declarations

Conflict of interest The authors declare no competing interests.

References

1. N. Schneider, L. Bonne, S. Bontemps et al., Ionized carbon as a tracer of the assembly of interstellar clouds. Nat. Astron. **7**, 546–556 (2023)
2. A. Poglitsch et al., The photodetector array camera and spectrometer (PACS) on the Herschel space observatory. A&A **518**, L2 (2010)
3. V. Revéret, et al. "B-BOP: the SPICA imaging polarimeter." in Space Telescopes and Instrumentation 2020: Optical, Infrared, and Millimeter Wave. Vol. 11443. (SPIE, 2020) pp. 1082–1091
4. P.D. Atherton, N.K. Reay, J. Ring, T.R. Hicks, Tunable Fabry–Perot filters. Opt. Eng. **20**, 206805 (1981)
5. K.F. Renk, L. Genzel, Interference filters and Fabry–Perot interferometers for the far infrared. Appl. Opt. **1**(5), 643–648 (1962)

6. R. Ulrich, K.F. Renk, L. Genzel, Tunable submillimeter interferometers of the Fabry–Perot type. IEEE Trans. Microw. Theory Tech. **11**(5), 363–371 (1963)
7. R. Ulrich, Far-infrared properties of metallic mesh and its complementary structure. Infrared Phys. **7**(1), 37–55 (1967)
8. G.R. Davis, I. Furniss, W.A. Towlson, P.A.R. Ade, R.J. Emery, W.M. Glencross, D.A. Naylor, T.J. Patrick, R.C. Sidey, B.M. Swinyard, Design and performance of cryogenic, scanning Fabry–Perot interferometers for the long-wavelength spectrometer on the infrared space observatory. Appl. Opt. **34**, 92–107 (1995)
9. Douthit, Greg, et al. "Development of the Fabry–Perot interferometers for the HIRMES spectrometer on SOFIA." in *Millimeter, Submillimeter, and Far-Infrared Detectors and Instrumentation for Astronomy IX*. Vol. 10708 (SPIE, 2018), pp. 195–207
10. Pajot, P. Francois, et al. "Design and performances of a cryogenic Fabry–Perot for submillimeter astronomy." in *Cryogenic Optical Systems and Instruments X*. Vol. 5172 (SPIE, 2003), pp. 13–20
11. N. Neumann et al., Tunable infrared detector with integrated micromachined Fabry–Perot filter. J. Micro/Nanolithogr. MEMS MOEMS **7**(2), 021004 (2008)
12. F. Cothard, Nicholas, et al. "Optimizing the efficiency of Fabry–Perot interferometers with silicon-substrate mirrors. in "*Advances in Optical and Mechanical Technologies for Telescopes and Instrumentation III*. 10706:1520–1528 (2018)
13. S. Bounissou, *« On-chip » astronomical instrumentation: bringing polarimetric and spectroscopic capabilities to the detector level* (Université Paris-Saclay, Diss, 2019)
14. P.M. Fauchet, Porous Silicon Optical Label-Free Biosensors, in *Device Applications of Silicon Nanocrystals and Nanostructures*. ed. by N. Koshida. Nanostructure Science and Technology. (Springer, Boston, MA, 2009)
15. F. Abelès, "Optics of thin films", [Advanced Optical Techniques], 143–188 (1967)